Microscopic gel-liquid interfaces supported by hollow microneedle array for voltammetric drug detection

Patricia Vazquez, Grégoire Herzog, Conor O'Mahony, Joseph O'Brien, James Scully, Alan Blake, Cian O'Mathuna, Paul Galvin

Microscopic gel – liquid interfaces supported by hollow microneedle array for voltammetric drug detection

Patricia Vazquez[1,2*], Grégoire Herzog[3*], Conor O'Mahony[1], Joseph O'Brien[1], James Scully[1], Alan Blake[1], Cian O'Mathuna[1,2] and Paul Galvin[1,2]

[1]*Tyndall National Institute, Lee Maltings, Dyke Parade, Cork, Ireland*

[2]*Clarity Centre for Sensor Web Technologies*

[3] *LCPME UMR 7564, CNRS-Université de Lorraine, 405 Rue de Vandoeuvre, 54600 Villers-lès-Nancy, France*

Corresponding authors: Patricia Vazquez: patricia.vazquez@tyndall.ie, T: + 353 21 234 6647; Grégoire Herzog: gregoire.herzog@univ-lorraine.fr; T: + 33 3 83 68 52 54.

This document is a postprint. Final version has been published in *Sensors and Actuators B: Chemical,* 2014, *201*, 572-578 (https://doi.org/10.1016/j.snb.2014.04.080).

Abstract

This report describes a method for integration of a gel-liquid interface in hollow microneedles compatible with minimally invasive, electrochemical detection of drugs in vivo. The electrochemical sensor was characterised using cyclic voltammetry of tetraethyl ammonium. The experimental work demonstrated the detection of propranolol as a representative drug in physiological buffer with the microneedle system. A calibration curve for propranolol was built from measurements with differential pulse stripping voltammetry, indicating a sensitivity of 43 nA μM^{-1}, a limit of detection of 50 nM and a linear range between 50 – 200 nM.

Keywords

Microneedles, micro-interfaces, ITIES, β-blocker drug, minimally invasive, stripping voltammetry.

1. Introduction

The past 20 years have seen the development of microneedles as an alternative to traditional subcutaneous needles for transdermal delivery of substances that are of medical interest. Microneedles have been used for the delivery of pharmacological compounds [1] and for vaccination [2, 3]. Research efforts have also been devoted to extend the use of microneedles beyond their traditional purpose of drug delivery, as it was the case in the use of metalized microneedles for electroporation therapy [4].

Hollow microneedles applied onto the skin are able to extract interstitial fluid [5, 6], offering a solution for a minimally invasive sensor of biomarkers in bodily fluids. However, detection of biomarkers of interest is done off-line [7], which requires the extraction of interstitial fluid from the body. Regardless of the method of extraction, the concept is hindered by the need of high vacuum pressures (200-500 mm Hg) for the extraction and collection of fluid [6]. Additionally, the volumes of fluid collected are variable [6, 8] and little is known of the reliability of extraction in a continuous basis. In conclusion, the complexity of a sensor able to provide continuous information of biochemical analytes in a physiological fluid would be drastically reduced with a design that did not require the uptake of biological fluids.

The use of electrochemical sensors can be a solution for an on-line detection without the need of sample extraction. Furthermore, miniaturised electrochemical sensors are more sensitive than macroscopic sensors [9] and electrochemical instrumentation is relatively easily miniaturised [10]. Recently, hollow polymeric microneedle arrays were filled with microelectrodes and used for the amperometric detection of hydrogen peroxide, lactate, glutamate and glucose [11, 12].

We report here a novel sensor based on an array of hollow microneedles filled with an organogel able to sense ionic species in a physiological fluid. This platform takes advantage of the possibility to polarise the interface formed between the organogel, located inside the hollow microneedle, and the physiological fluid. Electrochemical sensors based on micro-interfaces between two immiscible electrolyte solutions (μITIES) have been developed in recent years [13, 14]. This electrochemical technique is based on ions transferring across a polarized liquid-gel interface upon application of a potential difference. Ion transfer from one phase to another gives rise

to a current that can be monitored. Silicon-based micro and nano ITIES have been developed for the detection of analytes that are not redox active molecules [15, 16]. Examples like detection of dopamine [17] and peptides [18, 19] show the potential of this technique as an alternative to traditional electrochemical techniques.

We propose the use of a novel diagnostic platform that combines a hollow microneedle array with electrochemical detection at μITIES. The presence of the μITIES in the inner bore of the microneedles offers several advantages: it avoids the need of fluid extraction, as the ions cross the gel-liquid interface due to the potential difference applied at the interface; additionally, the reduced dimensions of the interface enhance rapid diffusion of species, which improves detection limits of the analytes. This effect is illustrated in different works on μITIES [18-21] and even used for the development of bioanalytical sensors [22].

We have selected propranolol as a model analyte. This drug belongs to the β-adrenergic blocking group [23]; it reduces heart rate and blood pressure, which makes it useful for treatment of hypertension and chest pain related to heart failure (angina) [23]. Blood pressure and heart rate correlate with propranolol levels in plasma [24]. Therefore, its direct measure in a physiological matrix could be useful for correct drug dosage and the monitoring of patient response to treatment. Propranolol has already been detected by ion transfer voltammetry at μITIES at concentration levels that are physiologically relevant [25-27], thus allowing useful comparison with the results reported here.

We present also the characterisation of the silicon microneedle system by scanning electron microscopy (SEM) and cyclic voltammetry (CV) of tetraethyl ammonium (TEA^+). This model analyte has been used extensively in the characterization of ITIES, as it presents rapid and mechanistically simple transfers in these systems [28-31]. The array is then used for the detection of propranolol in physiological medium by differential pulse stripping voltammetry (DPSV).

2. Material and methods

2.1. Reagents

All the reagents were purchased from Sigma-Aldrich Ireland Ltd. and used as received except for 1,6-dichlorohexane (1,6-DCH) (Merck), that was purified according to the published procedure [32]. The organic electrolyte salt was prepared by metathesis of bis-(triphenylphosphoranylidene) ammonium chloride ($BTPPA^+$ Cl^-) and of potassium tetrakis(4-chlorophenyl)-borate (K^+TPBCl^-) to obtain BTPPATPBCl, following the published experimental procedure [33]. The organogel phase was prepared using purified 1,6-DCH and low molecular weight polyvinylchloride (PVC) 10:1 (v:w) [14]. For the experiments of propranolol detection at the µITIES array, the aqueous phase was composed of magnesium pyrophosphate (1.6 mg L^{-1}), carboxymethyl cellulose (4 g L^{-1}), urea (4 g L^{-1}), disodium hydrogen phosphate (0.6 g L^{-1}), anhydrous calcium chloride (0.6 g L^{-1}), potassium chloride (0.4 g L^{-1}), and sodium chloride (0.4 g L^{-1}).

2.2. Microneedle array-µITIES

The silicon microneedle arrays were fabricated using a combination of potassium hydroxide (KOH) wet-etching and Bosch dry-etching techniques [34, 35]; the final microneedle array is shown in the scanning electron micrograph of figure 1A. Briefly, square oxide/nitride masks were patterned using standard photolithography tools on a <100>, boron doped, 100 mm diameter monocrystalline silicon wafer. These masks are aligned with the <110> direction and the patterned silicon wafer is then etched in a 29 % w/v aqueous KOH solution. Convex corner mask undercut takes place, leading to the formation of two angled planes at each corner, which eventually intersect to form an octagonal microneedle. This needle is comprised of eight {263} planes, a base of {212} planes and has a height to base aspect ratio of 3:2.

To form hollow bores through the microneedles, a 3 µm Plasma-Enhanced Chemical Vapour Deposition (PECVD) oxide layer is deposited and patterned on the rear of the wafer to act as a hard mask; a 2 µm layer of aluminium is sputtered on the front side of the wafer to act as an etch stop layer. 50 µm diameter capillary conduits are

then micromachined from the back side of the wafer using a Surface Technology System (STS) ASE ICP dry etching tool incorporating Bosch dry etching technology; the etch gases are SF_6 and C_4F_8. Afterwards, the aluminium layer and thick oxide layers are stripped from the front and back sides of the wafer, respectively.

In the case of the array used, the 300 µm high microneedles were separated by 1 mm. The bore is of a cylindrical shape with a diameter comprised between 55 and 62 µm as it is shown on the scanning electron microscope (SEM) image of figure 1A.

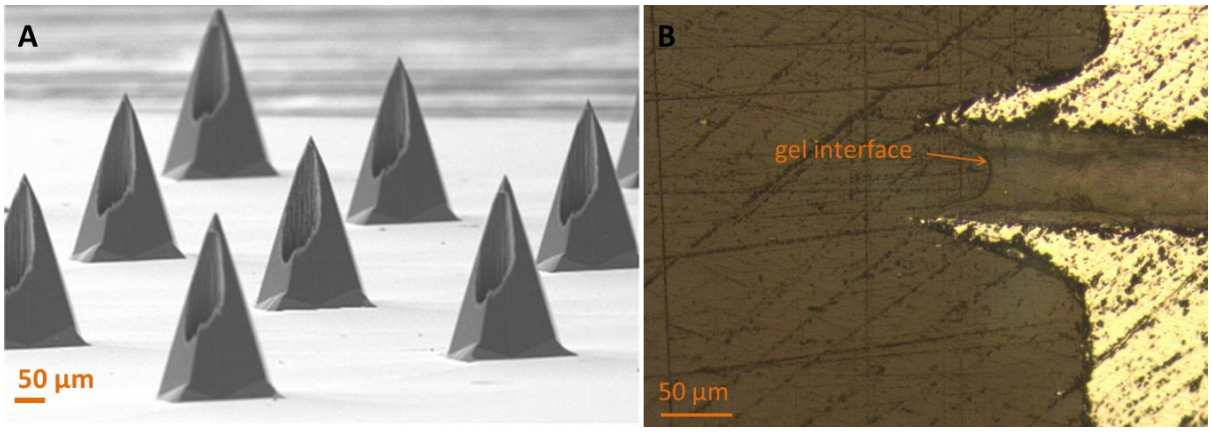

Figure 1: (A) SEM image of an array of hollow silicon microneedles. (B) Optical micrograph of the cross-section of a microneedle filled with the organogel. The microneedle system was encased in epoxy glue in order to facilitate subsequent slicing of the silicon material.

The creation of a micro ITIES at the microneedles is done by filling their bores with the organogel. A glass cylinder of 9 mm of inner diameter was sealed to the back of the microneedle array with silicone rubber. This configuration encloses a total of 52 hollow microneedles available for the experiments. The fabricated needles feature hydrophobic walls, which allowed an easy filling of the microneedle holes with the organogel; the latter had been heated gently at 50 °C in order to reduce its viscosity. The filling was done by pipetting the organogel onto the back of the microneedle array. Once the holes were filled (see figure 1B), the array was left to rest for at least 1 h before proceeding with the experiments.

2.3. Electrochemical set-up

In order to perform the electrochemical measurements, the system was configured as shown in figure 2.

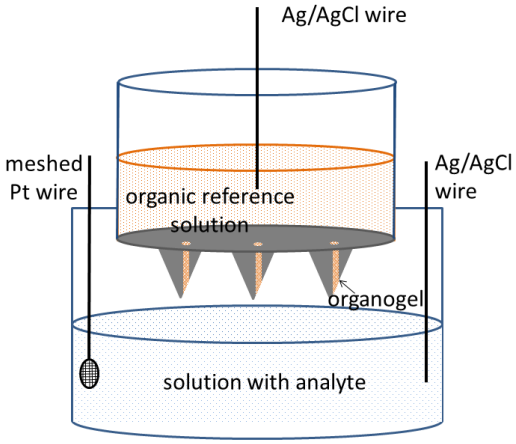

Figure 2: Experimental set up for electrochemical measurements. The aqueous phase consists of an Ag/AgCl wire and a meshed Pt wire as reference and counter electrodes respectively. Both are immersed in a solution with the analyte to be detected. As for the organic phase, a Ag/AgCl electrode behaves as both the reference and counter electrode.

The aqueous phase electrodes consisted of a platinum mesh counter electrode and a Ag/AgCl reference electrode. A Ag/AgCl wire acted as both the reference and counter electrode in the organic phase. The Ag/AgCl wires were prepared by oxidation of silver wires in a solution of $FeCl_3$. The aqueous phase electrodes are immersed in the beaker containing the aqueous solution, always clearly separated from each other. The electrode for the organic phase is immersed in the organic reference solution ($BTPPA^+TPBCl^-$). Finally, the microneedle-gel array is placed in the aqueous solution, making sure that the needles are completely immersed in the solution. Two electrochemical cells were used for these experiments. The first one, for the characterisation of the microneedle array by TEA^+ cyclic voltammetry, was as follows: Ag | AgCl | Saturated $BTPPA^+Cl^-$ in 10 mM LiCl | 10 mM $BTPPA^+TPBCl^-$ in 1,6 DCH-PVC organogel || 160 µM TEA^+ in 10 mM LiCl | AgCl | Ag. A second electrochemical cell was used for the detection of propranolol: Ag | AgCl | Saturated $BTPPA^+Cl^-$ in 10 mM LiCl | 10 mM $BTPPA^+TPBCl^-$ in 1,6 DCH-PVC organogel || different concentrations of propranolol in physiological buffer | AgCl | Ag.

For all experiments, the electrodes were connected to a CHI660B electrochemical analyser (CH Instruments, Texas, purchased from IJ Cambria, Burry Port, Wales, United Kingdom). Cyclic voltammetry was used as characterisation method, and differential pulse stripping voltammetry (DPSV) was chosen as the analytical detection method. The stripping method consisted of three steps: (i) preconditioning, (ii) preconcentration and (iii) detection. First, the ITIES went through an optimised preconditioning step during which a potential of 0.45 V was maintained for 120 s to clean the gel from any residuals of the analyte that may remain from a previous experiment. A preconcentration step was then used to transfer the analyte from the aqueous phase to the organic phase; the potential was held at 0.86 V for a period between 15 and 240 s to transfer the analytes to the organogel. These two steps allow concentrating the propranolol in the organogel. Finally, the detection step consisted of the back transfer of the preconcentrated propranolol to the aqueous phase by the scanning of a predefined potential window. The parameters for DPSV were: amplitude = 80 mV; pulse width = 0.1 s; sample width = 0.05 s; pulse period = 0.2 s. This DPSV protocol has been described previously [25].

3. Results and discussion

3.1. System characterization by cyclic voltammetry analysis

The electrochemical response of the hollow microneedle system was characterized by ion transfer voltammetry of the model analyte tetraethyl ammonium cation (TEA^+) at the ITIES formed in the bore of the needles. Before proceeding with any experiments, we determined the optimal scan rate values for the geometry of the needle array. The diffusion layer thickness (δ) should ideally be larger than the µITIES formed in the microneedles bores but not as large as to cause adjacent diffusion layers to overlap. This condition is highly desired as it results in the maximum faradaic current to background current ratio. To ensure non-overlapping diffusion areas between the holes of the array, it is sufficient to have $d > 2\delta$ [36], d being the distance of the holes from centre to centre.

The diffusion area can be approximated by Einstein's equation for the root mean-square displacement of diffusing particles with Brownian motions:

$$\delta = \sqrt{2D\,\Delta E/\nu} \quad (1)$$

In eq. (1), D is the diffusion coefficient ($m^2\ s^{-1}$); ΔE is the difference of potential between the onset of electrolysis and the peak of limiting current (V); ν is the scan rate ($V\ s^{-1}$). The substitution of this expression in the aforementioned condition for independent diffusion layers leads to the following equation for the scan rate:

$$\boldsymbol{\nu > 8D\,\Delta E/d^2} \quad (2)$$

In the particular case of our experiments, eq. (2) gives ν = 2.35 mV s^{-1} as the lower limit that present radial diffusion with no overlapping areas (taking $D = 9.8 \cdot 10^{-6}$ $cm^2\ s^{-1}$ for TEA^+ and ΔE = 0.3 V). All the experimental work was carried out with ν values higher than this limit. Therefore, the distance between adjacent microneedles (20 times the radius of the inner needle bore) is sufficiently large to avoid overlapping of the diffusion layer.

Figure 3A shows the cyclic voltammogram in the absence and in the presence of TEA^+ in the aqueous phase. In the absence of TEA^+, the potential window is limited by the transfer of the background electrolytes, noticeable in the steep variations of current at potentials greater than + 0.9 V and lower than + 0.2 V. The capacitance at + 0.6 V was estimated to be of (16.46 ± 0.40) µF cm^{-2}.

With the experiments conditioned as by the above calculations, asymmetry in the CVs was expected, as it has already been observed in a number of µITIES systems [37]. In these reported cases, a sigmoidal wave is observed in the forward scan, which results from the radial diffusion of species in the aqueous phase. On the other hand, the reverse scan showed a peak that corresponded to the linear diffusion of species inside the pores.

According to this, the microneedle system should present a steady state response during the forward sweep in the form of a sigmoidal curve for the TEA^+ transfer. However, as shown in figure 3A, it is hard to distinguish the TEA^+ transfer from the background electrolyte transfer. This could be explained by the hindered diffusion

towards the interface. The bore of the microneedle is not centred but slightly shifted to the side as it is shown in figure 1A and schematically represented in figure 3B. As a consequence, diffusion of species towards the micro-interface is not hemispherical as it can be observed at regular disk micro-interfaces. It presents a diffusion profile mixed between radial and linear as represented by the arrows in figure 3B.

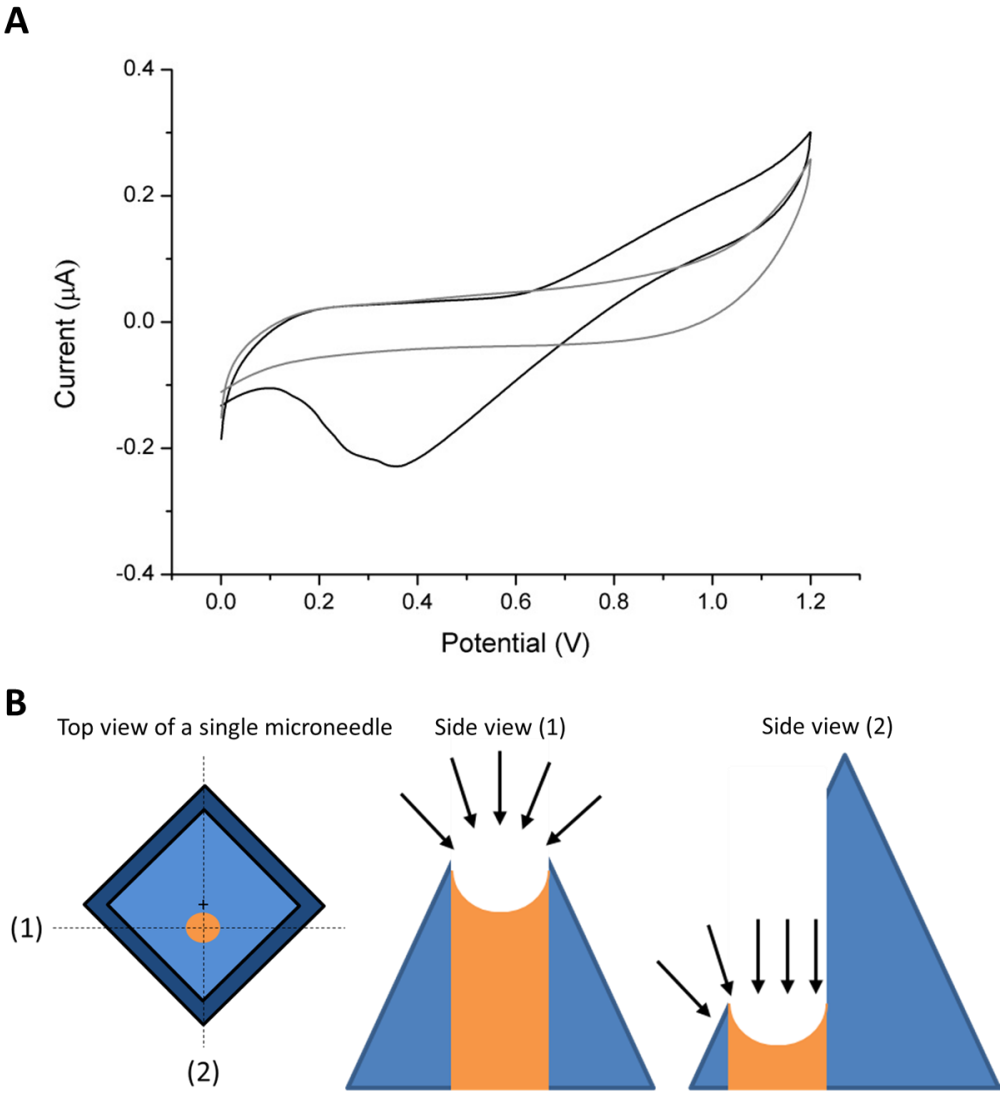

Figure 3: (A) Cyclic voltammetry curves in the presence (black) and in the absence (grey) of 160 µM TEA^+. The scan rate was 3.5 mV s^{-1}. (B) Schematic representation of the top view and side views of a microneedle filled with an organogel. The arrows represents the diffusion of species in the aqueous phase towards the organogel.

By contrast, the reverse sweep presents a peak-shaped voltammogram indicating a diffusion-controlled return of the analyte from the organic to the aqueous phase (see again figure 3). This was further corroborated by subsequent experiments where the

scan rate was varied between 5 and 17 mV s^{-1} (see figure 4). The measured reverse peak current is directly proportional (with R^2=0.997) to the square root of the scan rate, which confirms the presence of the diffusion-controlled process when TEA^+ transfers back to the aqueous phase.

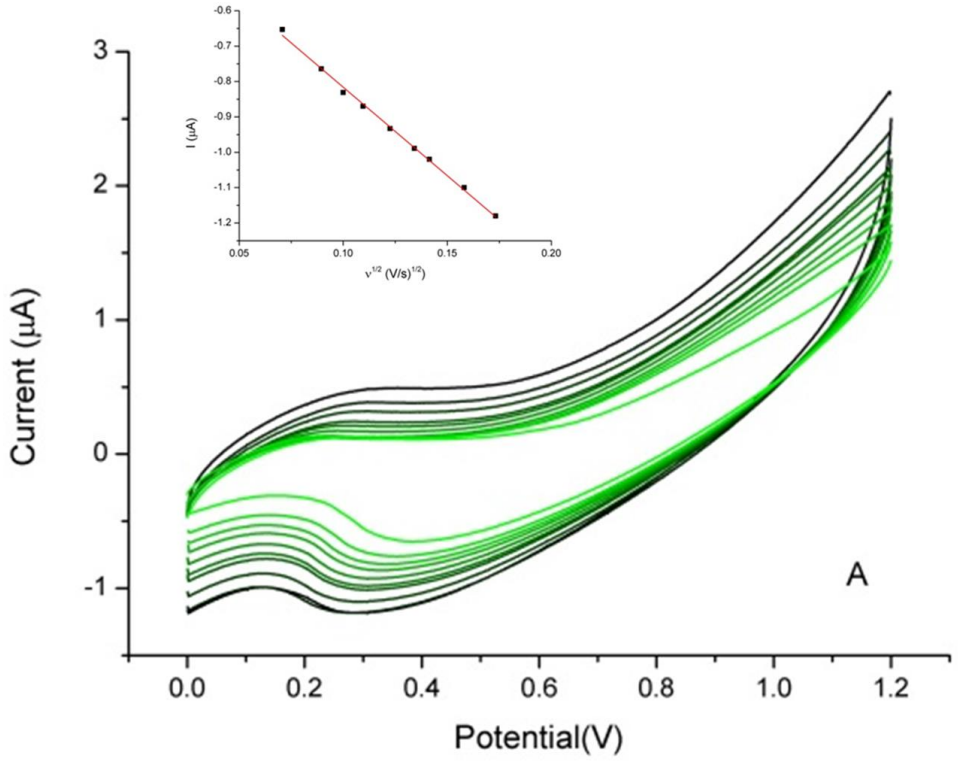

Figure 4: CVs of 160 μM TEA^+ in 10 mM LiCl, at increasing values of ν (5, 6, 7, 8, 9, 10, 11, 12, 15 and 17 mV/s; from light green to black, respectively). (Inset) Reverse current peaks against square root of ν. The peaks present a linear slope with the square root of ν, which is a typical response of diffusion-prevailing systems (R^2=0.997).

The gel phase forms a recessed interface at the aqueous side of the ITIES (as it can be seen in figure1B). Computational simulations have shown that this configuration is optimal for stripping voltammetry, as transport of analyte species to the gel micro-interface improves with a hemispherical diffusion regime during the preconcentration step [38] . Once they are transferred to the organic phase, they remain in the vicinity of the interface because of the reduced mass transport caused by both the linear diffusion and the lower diffusion coefficient in the PVC gel. Simulation studies have shown that the diffusion coefficient of TEA^+ was estimated to be nine times lower in the gel phase than in the aqueous solution [39].

3.2. Voltammetric detection of propranolol at the microneedle array

Figure 5 shows the CV of propranolol at the liquid-gel interface supported by the microneedle array. A sigmoidal wave is observed at + 0.7 V for the transfer of propranolol from the aqueous to the organic phase, whereas a peak is observed at + 0.25 V for the back transfer. The CV from propranolol shows the same features than with the experiments with TEA^+: hemispherical diffusion during the forward scan, and linear diffusion on the reverse sweep.

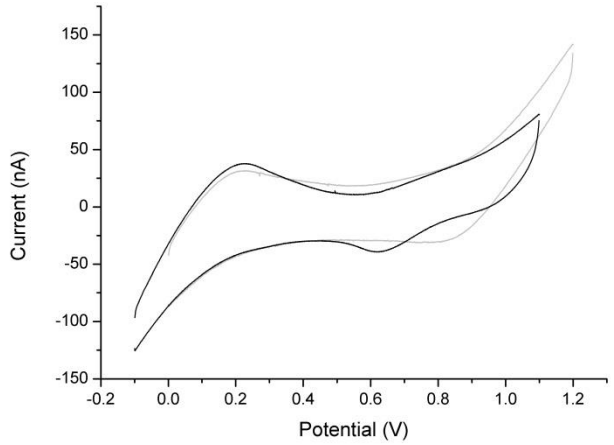

Figure 5: CV of 100 µM propranolol (black) and background electrolyte (grey). scan rate was 35 mV s^{-1})

The CV behaviour allows us to use eq. (3) to calculate the radius of the microneedle bore based on the propranolol limiting current, i_{lim}, measured on the forward scan.

$$i_{lim} = n4zFDCr \quad (3)$$

This equation defines the limiting current that is expected for an array of disc interfaces, where *n* is the number of microneedle interfaces (*n* = 52); *z* is the number of charge transferred (*z* = 1); F is the Faraday constant; *D* is the diffusion coefficient (D = 1.15 × 10^{-5} cm^2 s^{-1}, [40]); *C* is the propranolol concentration (C = 100 × 10^{-9} mol cm^{-3}) and *r* is the radius in cm. The theoretical limiting current of 57 nA (from equation 3) agrees well with the experimental value of 55 ± 3 nA (measured in CVs modified with background subtraction, not shown) corresponds to a microneedle interface radius of 25 µm, which agrees with the radius suggested by the SEM images (figure 1).

The use of differential pulse stripping voltammetry (DPSV) as the analytical technique offers the possibility to detect lower concentrations of the analyte as capacitive/background current is eliminated.

Figure 6 shows the DPSVs for increasing preconcentration times ranging from 15 to 240 s. Stripping peak currents increase slowly with the preconcentration time. Noticeably, the stripping peak current after 240 s of preconcentration is approximately 5 times higher than the one measured for 15 s. Based on these results, a preconcentration time t = 240 s was selected for the rest of experiments, as it provided the maximum current peak that was recorded.

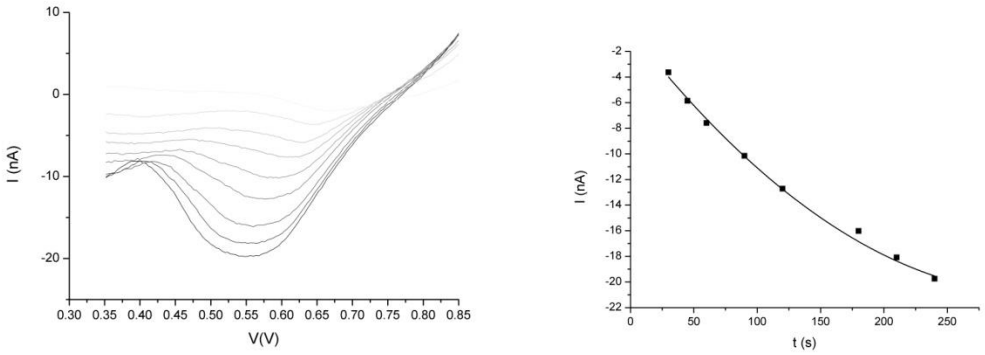

Figure 6:(A) DPSVs of 100 µM propranolol for increasing preconcentration times: 15, 30. 45, 60, 90, 120, 180, 210, 240 s. (B) Stripping peak current as a function of the preconcentration time

Once the preconcentration step was defined, DPSVs for increasing concentrations of propranolol in aqueous solution were recorded (figure 7A). The stripping peak (figure 7B) increased linearly with propranolol concentrations within the range 50 – 200 nM. A sensitivity of 43 nA μM^{-1} was calculated as the slope of the calibration curve (R^2 = 0.99423).

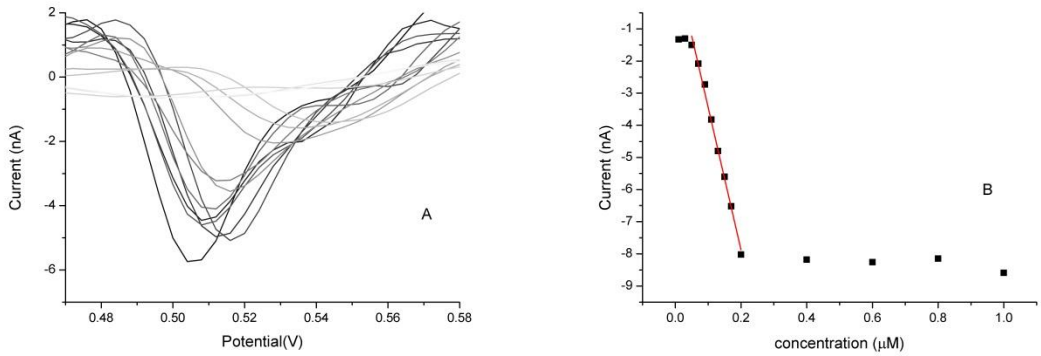

Figure 7: (A) DPSVs of different concentrations of propranolol in artificial saliva (propranolol concentrations, from lightest grey to black: 0.03, 0.05, 0.07, 0.09, 0.11, 0.13, 0.15, 0.17, 0.2, 0.4, 0.6,0.8 and 1 μM). (B) Current calibration curve for DPSVs of propranolol. Lower concentrations show a marked behaviour typical of spherical diffusion (a steep sloped line), whereas higher concentrations (typically, from 200 nM onwards) present a linear diffusion progress (flat line). R^2= 0.994.

The stripping peak for propranolol shifts towards less positive potential values as the preconcentration time or the concentration increase. This could be explained by two different phenomena (or a combination of both): (i) the kinetic limitation due to the increasing amounts of propranolol back-transferring or (ii) the uncompensated resistance due to an increasing ohmic drop. At concentrations higher than 200 nM, the stripping peak currents present a saturation effect. This could be justified by the fact that diffusion of propranolol is reduced due to the viscosity of the gel. The lowest concentration that the system was able to detect was 50 nM, which is within the detection limits published for propranolol [25, 43-46].

4. Conclusions

This report presents for the first time the development of a microneedle array with an embedded μITIES platform that is electrochemically able to detect propranolol. Although there is a wealth of literature reporting the use of μITIES for electrochemical detection, previous works were based in the use of micropipettes or arrays of micro and nano-holes as support structures for the miniaturized ITIES.

The array of sensors was capable of detecting propranolol in artificial saliva with good sensitivity and a limit of detection that is of pharmacological relevance. The use of miniaturized interfaces and DPSV as the analytical method of detection deliver a

low limit of detection, 50 nM, which compares well with previously published results for propranolol. This includes 0.2 µM with adsorptive stripping differential pulse voltammetry [47]; 5 µM for potentiometric membrane electrode [45]; 0.02 µM with cathodic adsorptive stripping voltammetry [48]; 0.1 µM for capillary electrophoresis [49]. The platform presents a linear range between 50 and 200 nM.

Our future line of work will address the application of the microneedle-µITIES system to the detection of biomarkers for *in vivo* applications. The characteristics of the microneedle-ITIES could be beneficial in a scenario for transdermal analysis, as the system can overcome the skin barrier with minimal pain (thanks to the microneedles) and without physiological fluid extraction (due to the µITIES embedded).
Nevertheless, the chemicals used for the organogel are toxic and will not be used as such for in-vivo applications. Future developments will need the investigation of new materials for the organic phase. We will look into compounds that present both biocompatibility and stability in the long term (the organogel presently used is volatile at air atmosphere and degrades slowly with time).
Additionally, even though the presence of the organogel in the bore of the needles should avoid potential clogging in transdermal applications, we will study this issue during future experimental work.

5. Acknowledgements

The authors would like to acknowledge support by Science Foundation Ireland (SFI) under grant 07/CE/I1147. P. Galvin would also like to acknowledge support from SFI through the INSIGHT, Biomedical Diagnostics and INFANT centres.

6. References

1. Wermeling, D.P., et al., *Microneedles permit transdermal delivery of a skin-impermeant medication to humans.* Proceedings of the National Academy of Sciences, 2008. 105(6): p. 2058-2063.
2. Van Damme, P., et al., *Safety and efficacy of a novel microneedle device for dose sparing intradermal influenza vaccination in healthy adults.* Vaccine, 2009. 27(3): p. 454-459.

3. Chabri, F., et al., *Microfabricated silicon microneedles for nonviral cutaneous gene delivery.* British Journal of Dermatology, 2004. 150(5): p. 869-877.
4. Wilke, N., et al., *Silicon microneedle electrode array with temperature monitoring for electroporation.* Sensors and Actuators A: Physical, 2005. 123–124(0): p. 319-325.
5. Mukerjee, E.V., et al., *Microneedle array for transdermal biological fluid extraction and in situ analysis.* Sensors and Actuators A: Physical, 2004. 114(2–3): p. 267-275.
6. Wang, P.M., M. Cornwell, and M.R. Prausnitz, *Minimally invasive extraction of dermal interstitial fluid for glucose monitoring using microneedles.* Diabetes Technol Ther, 2005. 7(1): p. 131-41.
7. Soller, B.R., et al., *Multiparameter Fiber Optic Sensor for the Assessment of Intramyocardial Perfusion.* Journal of Cardiac Surgery, 2004. 19(2): p. 167-174.
8. Stout, P.J., J.R. Racchini, and M.E. Hilgers, *A novel approach to mitigating the physiological lag between blood and interstitial fluid glucose measurements.* Diabetes technology & therapeutics, 2004. 6(5): p. 635-644.
9. Wang, J., *Portable electrochemical systems.* TrAC Trends in Analytical Chemistry, 2002. 21(4): p. 226-232.
10. Miller, P.R., et al., *Multiplexed microneedle-based biosensor array for characterization of metabolic acidosis.* Talanta, 2012. 88(0): p. 739-742.
11. Windmiller, J.R., et al., *Microneedle array-based carbon paste amperometric sensors and biosensors.* Analyst, 2011. 136(9): p. 1846-1851.
12. Malzahn, K., et al., *Wearable electrochemical sensors for in situ analysis in marine environments.* Analyst, 2011. 136(14): p. 2912-2917.
13. Herzog, G. and V. Beni, *Stripping voltammetry at micro-interface arrays: A review.* Analytica chimica acta, 2013. 769: p. 10-21.
14. Arrigan, D., *Bioanalytical detection based on electrochemistry at interfaces between immiscible liquids.* Analytical Letters, 2008. 41(18): p. 3233-3252.
15. Zazpe, R., et al., *Ion-transfer voltammetry at silicon membrane-based arrays of micro-liquid-liquid interfaces.* Lab on a Chip, 2007. 7(12): p. 1732-1737.
16. Scanlon, M.D., et al., *Ion-transfer electrochemistry at arrays of nanointerfaces between immiscible electrolyte solutions confined within silicon nitride nanopore membranes.* Anal Chem, 2010. 82(14): p. 6115-23.
17. Beni, V., M. Ghita, and D.W.M. Arrigan, *Cyclic and pulse voltammetric study of dopamine at the interface between two immiscible electrolyte solutions.* Biosensors and Bioelectronics, 2005. 20(10): p. 2097-2103.
18. Yuan, Y. and S. Amemiya, *Facilitated Protamine Transfer at Polarized Water/1,2-Dichloroethane Interfaces Studied by Cyclic Voltammetry and Chronoamperometry at Micropipet Electrodes.* Analytical Chemistry, 2004. 76(23): p. 6877-6886.
19. Herzog, G., et al., *Ion-Transfer Voltammetric Behavior of Protein Digests at Liquid|Liquid Interfaces.* Analytical Chemistry, 2009. 82(1): p. 258-264.
20. Scanlon, M.D., G. Herzog, and D.W.M. Arrigan, *Electrochemical Detection of Oligopeptides at Silicon-Fabricated Micro-Liquid/Liquid Interfaces.* Analytical Chemistry, 2008. 80(15): p. 5743-5749.
21. Herzog, G., et al., *Sensing via Voltammetric Ion-Transfer at an Aqueous-Organogel Micro-Interface Array.* Sensor Letters, 2011. 9(2): p. 721-724.
22. Pereira, C.M., et al., *Amperometric glucose biosensor based on assisted ion transfer through gel-supported microinterfaces.* Analytical Chemistry, 2004. 76(18): p. 5547-5551.
23. Baker, J.G., S.J. Hill, and R.J. Summers, *Evolution of β-blockers: from anti-anginal drugs to ligand-directed signalling.* Trends in Pharmacological Sciences, 2011. 32(4): p. 227-234.
24. Coltart, D.J. and D.G. Shand, *Plasma propranolol levels in the quaniitative assessment of beta-adrenergic blockade in man.* Br Med J, 1970. 3(5725): p. 731-4.

25. Collins, C.J. and D.W.M. Arrigan, *Ion-Transfer Voltammetric Determination of the β-Blocker Propranolol in a Physiological Matrix at Silicon Membrane-Based Liquid|Liquid Microinterface Arrays.* Analytical Chemistry, 2009. 81(6): p. 2344-2349.
26. de Eulate, E.A., L. Serls, and D.W. Arrigan, *Detection of haemoglobin using an adsorption approach at a liquid–liquid microinterface array.* Analytical and Bioanalytical Chemistry, 2013: p. 1-6.
27. Sisk, G.D., et al., *Assessment of ion transfer amperometry at liquid–liquid interfaces for detection in CE.* Electrophoresis, 2009. 30(19): p. 3366-3371.
28. Girault, H., *Charge Transfer across Liquid—Liquid Interfaces*, in *Modern Aspects of Electrochemistry*. 1993, Springer. p. 1-62.
29. Samec, Z. and T. Kakiuchi, *Charge Transfer Kinetics at Water-Organic Solvent Phase Boundaries*, in *Advances in Electrochemical Science and Engineering*. 2008, Wiley-VCH: p. 297-361.
30. Benjamin, I., *Molecular structure and dynamics at liquid-liquid interfaces.* Annual review of physical chemistry, 1997. 48(1): p. 407-451.
31. Wang, Y., et al., *Kinetic study of rapid transfer of tetraethylammonium at the 1, 2-dichloroethane/water interface by nanopipet voltammetry of common ions.* Analytical Chemistry, 2009. 82(1): p. 77-83.
32. Katano, H., H. Tatsumi, and M. Senda, *Ion-transfer voltammetry at 1, 6-dichlorohexane| water and 1, 4-dichlorobutane| water interfaces.* Talanta, 2004. 63(1): p. 185-193.
33. Lee, H.J. and H.H. Girault, *Amperometric Ion Detector for Ion Chromatography.* Analytical Chemistry, 1998. 70(20): p. 4280-4285.
34. C. O'Mahony, J.S., A. Blake, J. O'Brien, *A Microneedle-based Miniature Syringe for Transdermal Drug Delivery.* Proc. Micromechanics Europe, 2010.
35. J. O'Brien, M.B., A. Blake, J. Scully, E. Forvi, M. Casella, F. Gramatica, C. O'Mahony, *Hollow Microneedles for Pain-Free Drug Delivery.* Micromechanics Europe, 2009.
36. Davies, T.J. and R.G. Compton, *The cyclic and linear sweep voltammetry of regular and random arrays of microdisc electrodes: Theory.* Journal of Electroanalytical Chemistry, 2005. 585(1): p. 63-82.
37. Liu, S., Q. Li, and Y. Shao, *Electrochemistry at micro-and nanoscopic liquid/liquid interfaces.* Chemical Society Reviews, 2011. 40(5): p. 2236-2253.
38. Strutwolf, J. and D.W.M. Arrigan, *Optimisation of the conditions for stripping voltammetric analysis at liquid–liquid interfaces supported at micropore arrays: a computational simulation.* Analytical and Bioanalytical Chemistry, 2010. 398(4): p. 1625-1631.
39. Strutwolf, J., M.D. Scanlon, and D.W.M. Arrigan, *Electrochemical ion transfer across liquid/liquid interfaces confined within solid-state micropore arrays–simulations and experiments.* Analyst, 2009. 134(1): p. 148-158.
40. Fantini, S., et al., *Influence of the presence of a gel in the water phase on the electrochemical transfer of ionic forms of beta-blockers across a large water 1,2-dichloroethane interface.* Eur J Pharm Sci, 2003. 18(3-4): p. 251-7.
41. Zoski, C.G., et al., *Addressable microelectrode arrays: Characterization by imaging with scanning electrochemical microscopy.* Analytical Chemistry, 2004. 76(1): p. 62-72.
42. Ordeig, O., et al., *Regular arrays of microdisc electrodes: simulation quantifies the fraction of 'dead'electrodes.* Analyst, 2006. 131(3): p. 440-445.
43. Álvarez, A., et al., *Reusable phosphorescent probes based on molecularly imprinted polymers for the determination of propranolol in urine.* Sensors and Actuators B: Chemical, 2012. 168(0): p. 370-375.
44. Radi, A., A.A. Wassel, and M.A. El Ries, *Adsorptive behaviour and voltammetric analysis of propranolol at carbon paste electrode.* Chemia Analityczna, 2004. 49(1): p. 51-58.

45. El-Tohamy, M., M. El-Maamly, and A. Shalaby, *Propranolol hydrochloride-selective membrane electrode and their application to pharmaceutical preparations and biological fluids.* Bulletin of pharmaceutical sciences, 2006. 29(2): p. 488.
46. Ghoneim, M., A. Beltagi, and A. Radi, *Indirect determination of propranolol by cathodic adsorptive stripping voltammetry.* Quimica Analitica, 2002. 20: p. 237-241.
47. Sartori, E.R., et al., *Square-wave voltammetric determination of propranolol and atenolol in pharmaceuticals using a boron-doped diamond electrode.* Talanta, 2010. 81(4–5): p. 1418-1424.
48. Ghoneim, M.M., A.M. Beltagi, and A. Radi, *Indirect determination of propranolol by cathodic adsorptive stripping voltammetry.* Quimica Analitica, 2002. 20(4): p. 237-241.
49. Li, X., D. Zhu, and T. You, *Simultaneous analysis of six cardiovascular drugs by capillary electrophoresis coupled with electrochemical and electrochemiluminescence detection, using a chemometrical optimization approach.* Electrophoresis, 2011. 32(16): p. 2139-2147.
50. Collins, C.J., et al., *Serum-protein effects on the detection of the β-blocker propranolol by ion-transfer voltammetry at a micro-ITIES array.* Talanta, 2010. 80(5): p. 1993-1998.

7. Vitae

Patricia Vazquez is a postdoctoral researcher at Tyndall National Institute since 2011, where she is working as part of the Life Science Interface group in biomedical applications that require development of micro-electro mechanical systems (MEMS) and microfluidics. Dr. Vazquez graduated in Electronics from the University of Valencia (Spain) in 1999, and completed her PhD. in microfabrication from DTU (Danish Technical University) in 2010. Her current field of interest is the application of MEMS to neural studies.

Grégoire Herzog received his Ph.D. in Chemistry from University College Cork, Ireland in 2004. He then moved to Université Joseph Fourier in Grenoble, France. In 2005, he joined the Tyndall National Institute where he worked on the development of miniaturised electroanalytical tools based on ion transfer voltammetry at liquid–liquid interfaces. Since 2011, he is a researcher at the Laboratoire de Chimie Physique et Microbiologie pour l'Environnement (CNRS – Université de Lorraine, France) where he is working on the electrochemistry of liquid–liquid interfaces modified by silica thin films.

Dr. Conor O'Mahony is a Senior Research Scientist at the Tyndall National Institute, University College Cork, Ireland. He received the MEngSc and PhD degrees in 2000 and 2004, respectively, for the development of capacitive micro-switch technologies. He is currently responsible for the development of microneedle-based devices for a wide range of biomedical applications including transdermal delivery, diagnostics, electroporation and physiological signal monitoring. He has published over 140 papers in journals and at conferences, and has filed nine patent applications in the field of MEMS and micromachining. In 2012, he was Chair of the 2nd International Conference on Microneedles.

Joseph O'Brien is a senior process fabrication engineer with the Tyndall Microsystems Fabrication group. He received his B.Sc., in Chemistry in 1985 from University College Cork. His career at NMRC/Tyndall has involved working in all aspects of lithography from broadband to deep UV to electron beam lithography. He is currently working on advanced lithographic projects, focusing on high aspect ratio photo-resist fabrication routes for micromachining. Other areas of interest are the advanced silicon etching-BOSCH process and nano-imprinting on novel photoresists. He also leads the Microsystems wafer bonding facility.

James Scully received a B.Eng. in Electronics from the National Institute of Higher Education (NIHE) in Limerick. James has 20 years of experience in equipment and process engineering in the NMRC / Tyndall National Institute at University College Cork.

Alan Blake graduated from the University of Limerick with a B.Sc. (Applied Physics) and has worked as a process-engineer in the Central Fabrication Facility at Tyndall National Institute since 2000 with responsibility for a number of areas within the Silicon-Fabrication group, including photolithography, etch, PECVD and ALD. Research interests include CMOS and MEMS processing and technology development.

Prof. Cian Ó Mathúna is Head of the Microsystems Centre at Tyndall National Institute, and a Research Professor in the department of Electrical and Electronic Engineering, University College Cork. With more than 30 years' experience in applied research and technology transfer to industry, his investigation has focused

on CMOS microsystems that provide intelligent platforms of non-standard functions such as sensors, actuators, power and cooling.

In January 2013, he was named an IEEE Fellow in the field of power electronics “for leadership in the development of power supply using micro-magnetics on silicon”.

Dr. Paul Galvin was awarded his PhD in 1995 and joined the Tyndall National Institute (then NMRC) in 2000, where he now leads the Life Sciences Interface Group. Research within his group is focussed on exploiting the extensive design, fabrication and characterisation tools available in Tyndall, for applications related to health and environment. Dr Galvin is a PI in the Science Foundation Ireland INFANT centre, collaborates in the SFI BDI and INSIGHT centres, and has led two international multidisciplinary research projects. He has over 60 international publications, and has presented his research at numerous international conferences.

Captions

Figure 1: (A) SEM image of an array of hollow silicon microneedles. (B) Optical micrograph of the cross-section of a microneedle filled with the organogel. The microneedle system was encased in epoxy glue in order to facilitate subsequent slicing of the silicon material.

Figure 2: Experimental set up for electrochemical measurements. The aqueous phase consists of an Ag/AgCl wire and a meshed Pt wire as reference and counter electrodes respectively. Both are immersed in a solution with the analyte to be detected. As for the organic phase, a Ag/AgCl electrode behaves as both the reference and counter electrode.

Figure 3: (A) Cyclic voltammetry curves in the presence (black) and absence (grey) of 160 µM TEA+, for an array of 56 micropores/needles. The scan rate was 35 mV s^{-1}. (B) Schematic representation of the top view and side views of a microneedle filled with an organogel. The arrows represent the diffusion of species in the aqueous phase towards the organogel. The addition of 160 µM TEA^+ to the aqueous solution leads to an increase of the current starting from + 0.6 V, indicating the TEA^+ transfer. On the reverse scan, a peak is visible at + 0.4 V, corresponding to the transfer of the TEA^+ from the organic phase back to the aqueous phase.

Figure 4: CVs of 160 µM TEA+ in 10 mM LiCl, at increasing values of ν(5, 6, 7, 8, 9, 10, 11, 12, 15 and 17 mV s^{-1}; from light green to black, respectively). The experiments correspond to an array of needles with 56 micropores. (Inset) Reverse current peaks against square root of ν. The peaks present a linear slope with the square root of ν, which is a typical response of diffusion-prevailing systems (R^2=0.997).

Figure 5: CV of 100 µM propranolol (black) and background electrolyte (grey). Scan rate was 8 mV s^{-1}).

Figure 6: (A), DPSVs of 100 µM propranolol for increasing preconcentration times: 15, 30. 45, 60, 90, 120, 180, 210, 240 s. (B), Stripping peak current as a function of the preconcentration time.

Figure 7: (A) DPSVs of different concentrations of propranolol in artificial saliva. (B) Corresponding current calibration curve for DPSVs of propranolol. Measurements were performed for the following concentrations of propranolol: 0.03, 0.05, 0.07, 0.09, 0.11, 0.13, 0.15, 0.17, 0.2, 0.4, 0.6, 0.8 and 1 µM (figure A shows a selection of plots for visual clarity, corresponding to concentrations of propranolol of 0.07, 0.09, 0.11, 0.15, 0.17, 0.2, 0.8 and 1 µM). Lower concentrations show a marked behaviour typical of spherical diffusion (a steep sloped line), whereas higher concentrations (typically, from 200 nM onwards) present a linear diffusion progress (flat line). R^2= 0.994.